Eur. Phys. J. B **40**, 305–312 (2004)
DOI: 10.1140/epjb/e2004-00271-1

THE EUROPEAN PHYSICAL JOURNAL B

Study of a monomer-monomer reaction system with short-range repulsive interactions

Monomer-monomer reaction system with repulsive interactions

M.A. Sanservino[1], A. López[1], E.V. Albano[1], and R.A. Monetti[2,a,b]

[1] Instituto de Investigaciones Fisicoquímicas Teóricas y Aplicadas, (INIFTA), CONICET, UNLP. Sucursal 4, Casilla de Correo 16, (1900) La Plata, Argentina
[2] Center for Interdisciplinary Plasma Science (CIPS), Max Planck-Institut für extraterrestrische Physik, Giessenbachstr. 1, 85748, Garching, Germany

Received 24 March 2004 / Received in final form 8 July 2004
Published online 31 August 2004 –

Abstract. The critical behavior of an interacting two species catalytic surface reaction model is studied by means of Monte Carlo simulations and a mean-field approach. The model has two parameters, namely the relative adsorption rate of species p_A and a short-range repulsive interaction r between the same type of adsorbed species. The system exhibits an stationary reactive phase and two symmetrically equivalent absorbing phases. These latter phases are unique and correspond to surfaces saturated by a single type of reacting species. For $r > 0 \wedge r \neq 1$, the system exhibits a second-order phase transition that belongs to the directed percolation (DP) universality class. However, in the absence of repulsive interaction ($r = 0$), a bicritical point is found at $p_A = 1/2$ whose critical behavior is compatible with dynamical mean-field exponents. Our findings indicate that the bicritical point belongs to the Voter Model universality class, whose upper critical dimension is $d_c = 2$. In addition, we propose a method to study the crossover from MF to DP behavior based on the estimation of the crossover time T_c. We find that T_c diverges according to a power-law $T_c \propto r^{-\mu}$ as $r \to 0$ where $\mu \simeq 1.17 \pm 0.03$ is the crossover exponent. For strong repulsion, a new transient effect appears associated with the onset of almost inactive "chessboad" patterns.

PACS. 02.50.-r Probability theory, stochastic processes, and statistics – 05.40.-a Fluctuation phenomena, random processes, noise, and Brownian motion – 82.45.Jn Surface structure, reactivity and catalysis

1 Introduction

Very recently, the study of non-equilibrium surface reaction systems has attracted growing attention. This interest is motivated by both their technological applications and their academic and scientific relevance. Examples of technical applications include the manufacture of chemicals via heterogeneously catalyzed reactions, the treatment of automobile exhausts, the reduction of environmental pollution, coating, corrosion and passivation of surfaces, synthesis and refinement of hydrocarbons, etc. On the other hand, the scientific interest arises out of the emergency of rich and complex physical and physical-chemistry phenomena including, chaos, bistability, critical phenomena and irreversible phase transitions, propagation and interference of chemical waves of adsorbed reactants, chemicals oscillations, etc. [1–5].

From the scientific point of view, an approach to treat these complex reaction systems is to study simple lattice gas models by means of numerical Monte Carlo simulations complemented by mean-field treatments [4,5]. These methods are very useful because one lacks of a well established theoretical framework since the development of the statistical mechanics of far-from equilibrium chemical reactions is in its infancy. In fact, it is known that lattice gas reaction models for elementary reactions such as the catalytic oxidation of carbon monoxide [6], the catalyzed reaction CO + NO [7], the catalytic oxidation of hydrogen [8,9], etc. (for reviews see [5,10]) exhibit both first- and second-order irreversible phase transitions (IPT's). In contrast to their reversible counterpart, where each phase can reversible be reached by tuning a suitable parameter, IPT's take place between an active state (or reactive regime with sustained production of desorbing molecules) and an inactive (or poisoned) state where the reaction stops due to the irreversible saturation of the catalytic surface by one or more reactants. Notice that the physical system can not escape from a poisoned state where it is

[a] e-mail: roberto@cips.mpg.de
[b] *Permanent address*: Instituto de Investigaciones Fisicoquímicas Teóricas y Aplicadas, (INIFTA), CONICET, UNLP. Suc. 4, C. C. 16, (1900) La Plata, Argentina

trapped forever, so the poisoned state is also known as an absorbing state of the system.

Within this context, the aim of the present work is to study the critical behavior of the Zhuo, Park and Redner (ZPR) model [11] in $d = 2$ dimensions. The ZPR model, which has early been studied in $d = 1$ [11] corresponds to a monomer-monomer reaction system with short-range repulsive interactions. Our study, which is based on both numerical Monte Carlo Simulations and a Mean Field (MF) approach, reveals a rich critical behavior, qualitatively different to that observed in the $d = 1$ case, as discussed in detail below. The manuscript is organized as follow: the ZPR model is defined in Section 2; the Monte Carlo simulation method and the Mean Field approach are described in Sections 3.1 and 3.2, respectively. Results are presented and discussed in Section 4 and the conclusions are stated in Section 5.

2 The ZPR model

The ZPR model considers the surface catalyzed reaction of two kind of monomers A and B, respectively. The arrival probability of A (B)-species to the surface is p_A (p_B), respectively, such as $p_A + p_B = 1$. The repulsive interaction between the **same kind** of monomers on nearest neighbor (NN) sites is accounted by a " repulsion " parameter r with $(0 \leq r < 1)$. Therefore, the adsorption on an empty site surrounded by an empty neighborhood proceeds with probability p_A or p_B, depending on the adsorbing species. However, the adsorption probability on a certain empty site that has at least a single NN site occupied by the same species is weakened by a factor $(1 - r)$. Summing up, the ZPR model has two independent parameters: p_A and r. It is assumed that the reaction proceeds according to the Langmuir-Hinshelwood mechanism, that is with both reactants adsorbed on the surface, so:

$$A(g) + S \rightarrow^{k_A} A(a) \quad (1)$$

$$A(g) + S' \rightarrow^{k'_A} A(a) \quad (2)$$

$$B(g) + S \rightarrow^{k_B} B(a) \quad (3)$$

$$B(g) + S' \rightarrow^{k'_B} B(a) \quad (4)$$

$$A(a) + B(a) \rightarrow^{k_R} (AB) \uparrow + 2S \quad (5)$$

where $A(g)$ and $B(g)$ are particles in the gas phase, $A(a)$ and $B(a)$ are adsorbed particles, and S $(S^{'})'$ is an empty site of the lattice such as none (at least one) of their NN sites are (is) occupied by the same species. The molecule $(AB) \uparrow$ is the reaction product that leaves the surface causing the re-generation of empty sites. The adsorption rate constants are $k_A = p_A$, $k_A^{'} = (1 - r)\, p_A$, $k_B = 1 - p_A$, and $k_B^{'} = (1 - r)\,(1 - p_A)$ where the relationship $p_A + p_B = 1$ has been used. Reaction between NN adsorbed species of different type is instantaneous ($k_R \rightarrow \infty$ in Eq. (5)), i.e. the reaction is controlled by adsorption,

$$k_R \gg k_A,\, k_B,\, k'_A,\, k'_B. \quad (6)$$

In $d = 1$, Zhuo et al. [11] have shown that for $0 \leq r < r_c \cong 0.2565$ the ZPR model exhibits a line of first-order IPT's which separates absorbing states saturated by different species, while above the bicritical point r_c ($r > r_c$) this line bifurcates and a finite-width reaction window is observed.

3 Numerical approaches

3.1 The Monte Carlo simulation method.

The ZPR model is simulated in $d = 2$ dimensions on the square lattice using samples of side L and assuming periodic boundary conditions. The lattice side L is measured in lattice units (LU). Double occupancy of a lattice sites is forbidden. The time unit is given by the Monte Carlo time step (mcs) that involves $L \times L$ adsorption trials, so that each site of the lattice is visited once, on the average.

Preliminary runs of the standard Monte Carlo algorithm indicate that in $d = 2$, the ZPR model exhibits second-order IPT's. So, in order to obtain accurate values of the critical points and to determine the universally class, epidemic simulations (ES) [12,13] were performed. The basic concept behind an ES is to initialize the simulation using a configuration very close to the poisoned (absorbing) state. For the case of the state poisoned by A-species, this kind of configuration is simply obtained by covering the whole lattice with A-monomers, except for a small patch of empty sites located at the center of the sample for computational convenience. In this paper, most of the results are obtained using patches consisting of a single empty site. Runs initialized using patches of different size show the same asymptotic properties. After initializing the system, the ES actually starts and the time evolution of the system is monitored through the following quantities: (i) the average number of empty sites ($N(t)$); (ii) the survival probability of the epidemics ($P(t)$), that is the probability that reactions still occur at time t; and (iii) the average square distance of the empty sites relative to the center of the starting epidemics ($R^2(t)$) [12,13]. Of course, each single ES finishes when the system is trapped in the poisoned state ($N(t) = 0$). Results are averaged over 10^5 different epidemics. It should be noticed that $N(t)$ is averaged over the total number epidemics while $R^2(t)$ is averaged only over surviving epidemics.

Close to a second-order phase transition $P(t)$, $N(t)$ and $R^2(t)$ exhibit power-law behavior and the following Ansätze are expected to hold [12,13]:

$$P(t) \propto t^{-\delta}, \quad (7)$$

$$N(t) \propto t^{\eta}, \quad (8)$$

and

$$R^2(t) \propto t^{z}, \quad (9)$$

where δ, η and z are dynamic critical exponents. All these exponents are related through an hyper-scaling relationship given by [12,13]

$$dz = 4\delta + 2\eta. \quad (10)$$

As expected, the scaling laws given by equations (7, 8, 9) are only valid at criticality. So, using log-log plots of the numerical data it is possible to evaluate not only the dynamical critical exponents but also to determine the critical point, since upward and downward deviations from linearity are observed within the reactive and poisoned regimes, respectively. Lattices are taken large enough to prevent the epidemics to reach the boundaries of the samples. Therefore, exponents determined using ES are free of undesired finite-size effects.

3.2 A mean field approach

Mean Field (MF) treatments of reaction models usually gives a rough insight on the behavior of the system. In fact, since all quantities under consideration are averaged over the whole sample, the MF approach neglects fluctuations and long-range correlations that are essential for a correct description of continuous transitions.

In this work, a set of single-site MF equations is obtained for the time evolution of the densities $\rho_A(t)$ and $\rho_B(t)$. The density of a given species increases (decreases) due to adsorption (reaction following desorption) events. So, the generic MF equations can be written as:

$$\frac{d\rho_A}{dt} = \sum_{i=1}^{5} m_i^a f_{ai}^A - \sum_{j=1}^{10} m_j^d f_{dj}^A, \tag{11}$$

where f_{ai}^A and f_{dj}^A are the occurrence probability of adsorption (a), and desorption (d), respectively. m_i^a and m_j^d are multiplicity factors corresponding to the neighbor configurations. For instance, let us focus on the adsorption term in equation (11). There are five different neighbor configurations ($i = 1, \cdots, 5$) namely, an empty neighborhood ($m_1^a = 1$), a neighborhood having one A-particle ($m_2^a = 4$), a neighborhood having two A-particles ($m_3^a = 6$), a neighborhood having three A-particles ($m_4^a = 4$), and a neighborhood having four A-particles ($m_5^a = 1$). For the desorption term, more configurations are possible since the neighborhood may have also B-particles. For the particular case of A-species, equation (11) can be written as:

$$\begin{aligned}\frac{d\rho_A}{dt} &= p_A\rho_V^5 + (p_A r\rho_V - p_B\rho_V)\rho_A^4 + 4(p_A r\rho_V - p_B\rho_V \\ &\quad - p_B r\rho_B)\rho_V\rho_A^3 + 6\rho_V\rho_A^2(p_A r\rho_V^2 - p_B\rho_V^2 \\ &\quad - 2p_B r\rho_V\rho_B - p_B r\rho_B^2) + 4\rho_V\rho_A(p_A r\rho_V^3 - p_B\rho_V^3 \\ &\quad - 3p_B r\rho_V^2\rho_B - 3p_B r\rho_V\rho_B^2 - p_B r\rho_B^3). \end{aligned}\tag{12}$$

There is also an analogous equation for B particles, namely

$$\frac{d\rho_B}{dt} = \sum_{i=1}^{5} m_i^a f_{ai}^B - \sum_{i=1}^{10} m_i^d f_{di}^B \tag{13}$$

The set of equations (11) and (13) has to be solved with the constraint

$$\rho_A + \rho_B + \rho_V = 1, \tag{14}$$

where ρ_V is the density of empty sites.

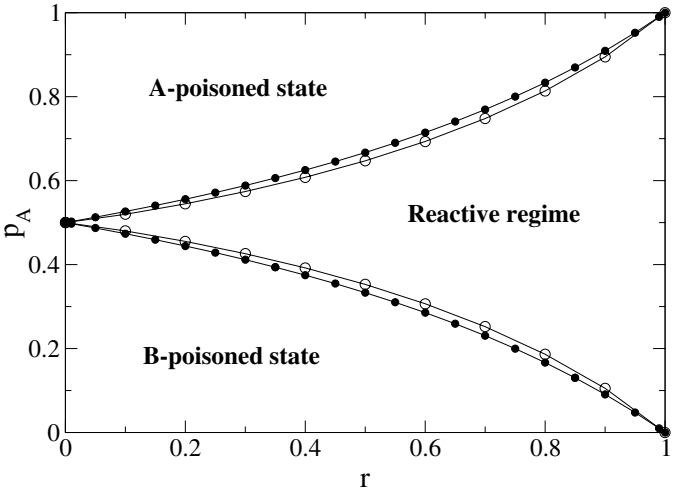

Fig. 1. Phase diagram of the ZPR model in $d = 2$ dimensions. The symbols ∘ and • correspond to MF results and epidemic Monte Carlo dynamic simulations, respectively.

4 Results and discussion

Solving the MF equations numerically, it is possible to determine the critical points where the system undergoes IPT's. The obtained phase diagram, shown in Figure 1, exhibits the expected particle exchange symmetry. Three phases can be easily distinguished, namely a reactive regime and two poisoned states with A and B species, respectively.

After obtaining a first insight on the behavior of the system with the MF analysis, we have proceeded to perform extensive Monte Carlo simulations. Figure 2 shows data corresponding to ES for $r = 0$ and $p_A = 1/2$. As shown in Figure 2a, power laws are obtained for all measured quantities namely, $N(t)$, $P(t)$, and $R(t)$, as expected from equations (7, 8) and (9), respectively. Accurate values of the exponents can be obtained measuring the time dependence of effective exponents given by [13]:

$$-\delta_{\mathit{eff}}(t) = \frac{\log_{10}\left(P(t)/P(t/\tau)\right)}{\log_{10}(\tau)}, \tag{15}$$

where τ is the time interval used to compute the effective exponents. All the simulations have been performed using $\tau = 5$. Notice that similar relationships can be written for both $\eta_{\mathit{eff}}(t)$ and $z_{\mathit{eff}}(t)$ [13]. The temporal evolution of the effective exponents are shown in Figure 2b. By performing a mean-square fit of the results shown in Figure 2a and $t \to \infty$ extrapolations of the data shown in Figure 2b, our estimations of the exponents are $\eta = -0.03(3)$, $\delta = 0.98(2)$ and $z = 1.04(4)$. So, it is concluded that for this particular point of the phase diagram at $p_A = 1/2$ and in the absence of repulsion ($r = 0$), the exponents correspond to the well known MF behavior with $\eta = 0$, $\delta = 1$ and $z = 1$ [14], respectively.

On the other hand, considering repulsion ($r > 0$), the dynamical critical behavior is quite different, as shown in Figure 3 for $r = 0.2$. In fact, in this case the obtained exponents are $\eta = 0.214(5)$, $\delta = 0.48(2)$ and $z = 1.125(5)$.

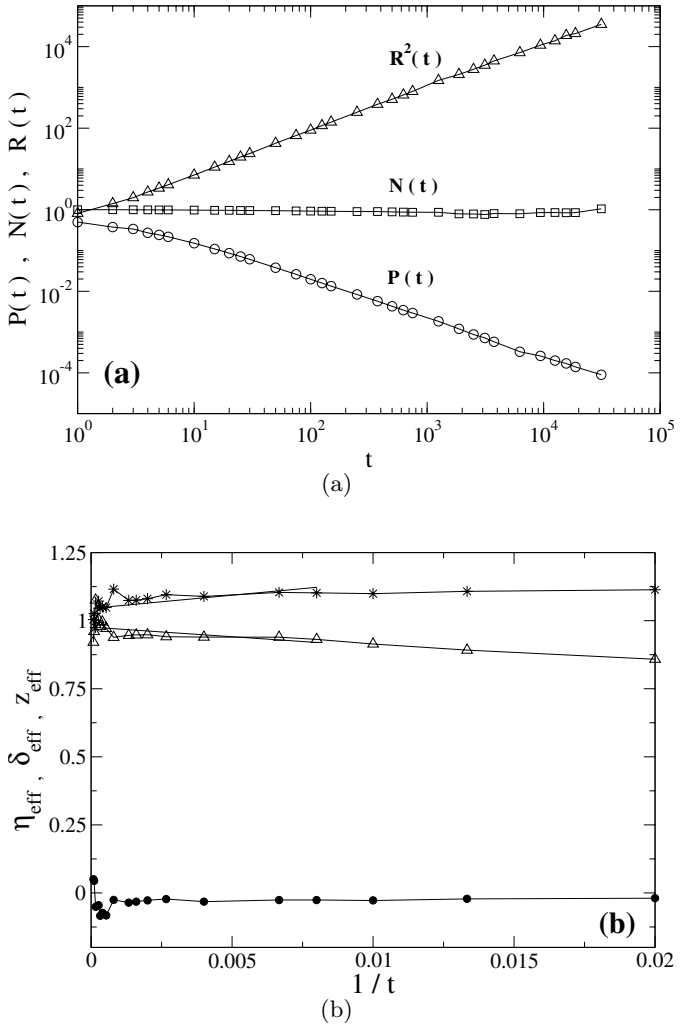

Fig. 2. Results of ES obtained for $r = 0$ and $p_A = 1/2$. The results are averaged over 10^6 different runs. (a) Log-log plots of: $R^2(t)$, $N(t)$, and $P(t)$ vs. time. (b) Plots of the effective exponents η_{eff}, δ_{eff}, and z_{eff} vs. $1/t$. The time is measured in mcs. The extrapolations to $t \to \infty$ give the estimations of the critical exponents quoted in the text.

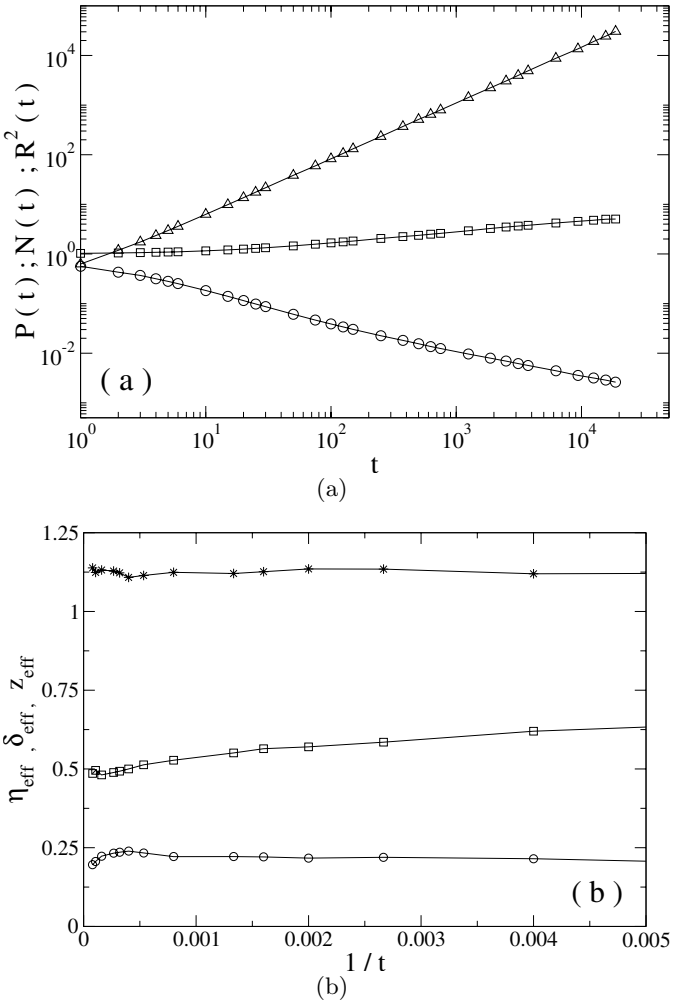

Fig. 3. Results of ES for $r = 0.2$. The results are averaged over 10^5 different runs. (a) Log-log plots of $N(t)$, $P(t)$ and $R^2(t)$ vs. time. A power-law behavior for all these quantities is obtained for $p_A = 0.5447$, while sub-critical and super-critical deviations are observed otherwise (not shown here for the sake of clarity). (b) Plots of the effective exponents η_{eff}, δ_{eff} and z_{eff} vs. $1/t$. The time is measured in mcs. The extrapolations to $t \to \infty$ give the estimations of the exponents quoted in the text.

Notice that these exponents satisfy the hyperscaling relationship given by equation (10) with $d = (4\delta + 2\eta)/z = 2.09 \pm 0.03$.

Furthermore, within the poisoned state it is expected that $N(t)$ would decay exponentially, so

$$N(t) \propto \exp(-\lambda(p_A)\, t), \tag{16}$$

where the factor $\lambda(p_A)$ behaves as

$$\lambda(p_A) \propto (p_A - p_{Ac})^{\nu_\parallel}, \tag{17}$$

where $\nu_\parallel$ is the critical exponent of the temporal correlation length. Therefore, after an accurate estimation of the critical point, it is possible to evaluate $\lambda(p_A)$ by measuring the time decay of $N(t)$ for different values of p_A. Subsequently, log-log plots of λ vs. $(p_A - p_{Ac})$ allow the evaluation of $\nu_\parallel = 1.23(5)$ (see Fig. 4).

It should be noticed that all the evaluated exponents are in excellent agreement with those corresponding to the directed percolation (DP) universality class in $(2+1)$ dimensions, given by $\delta = 0.4505(1)$, $\eta = 0.2295(1)$, $z = 1.1325(1)$ and $\nu_\parallel = 1.295(6)$ [14,15].

Epidemics studies, similar to those presented here for $r = 0.2$, have also been performed for several values of the repulsion parameter. The obtained critical exponents for $r > 0$ are always in excellent agreement with those of the DP, i.e. the critical curve belongs to the DP universality class. Figure 1 shows the phase diagram of the ZPR model in 2-dimensions. It is worth mentioning that the phase diagram obtained using the single site MF approach is in good agreement with that obtained by means of Monte Carlo simulations. This agreement is remarkable

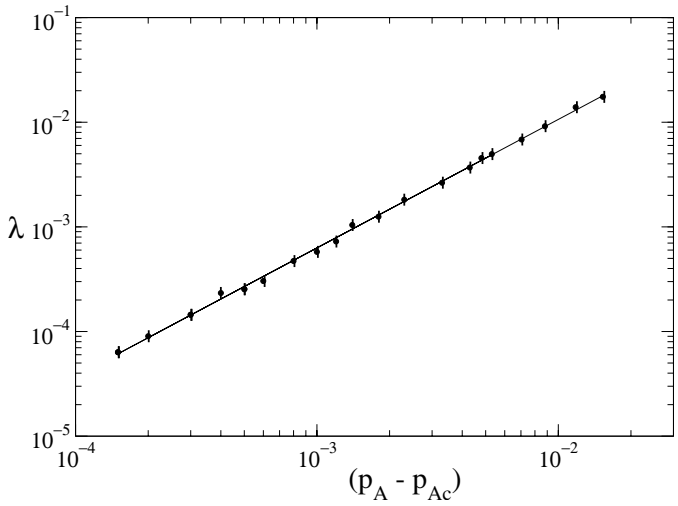

Fig. 4. Log-log plot of λ vs. $p_A - p_{Ac}$, as obtained for $p_{Ac} = 0.5447$. The straight line has slope $\nu_{\parallel} = 1.23$ and corresponds to the best fit of data.

considering the rough approximations introduced in the derivation of the MF equations.

Summing up, the phase diagram of the ZPR model in d=2 dimensions exhibits a mean-field like critical point at $(p_A = 1/2, r = 0)$, while for $r > 0$ the (symmetric) critical lines correspond to second-order IPT's that belong to the DP universality class. On view of this finding, we have analyzed the crossover from MF to DP behavior as well. In fact, Figure 5 shows log-log plots of $N(t)$ versus t obtained at criticality for different values of r. It is found that for $r \to 0$ ($r = 0.005$ in Fig. 5) the dynamical behavior is controlled by the bicritical point (MF like behavior) for short times, subsequently changing to DP behavior. The crossover time (T_c) as defined in Figure 5 is $T_c \cong 650$ mcs. As expected, T_c decreases when increasing r, i.e. away from the MF critical point. This behavior can be observed in the inset of Figure 5 which shows a log-log plot of T_c versus r_c. For $r_c \leq 0.1$ a power-law decay of the form

$$T_c \propto r_c^{-\mu}, \tag{18}$$

is found and the best fit of the data gives $\mu = 1.17(3)$. The observed decay-law suggest a scaling plot of $N(t)$ versus t/T_c as shown in Figure 6. The obtained data collapsing is excellent and strongly supports an unified description of the dynamical crossover behavior for different values of the repulsion parameter. On the other hand, it is also expected that near the bicritical point, the border of the active phase behaves as $(p_{Ac} - 0.5) \propto r_c^{\phi}$, where ϕ is the crossover exponent [16]. The inset of Figure 6 shows a log-log plot of $(p_{Ac} - 0.5)$ versus r_c along the reactive phase edge near the bicritical point. We obtain a crossover exponent $\phi \sim 1.13(3)$, which indicates that $\phi = \mu$ within the error bars. Consequently, the crossover time diverges at the bicritical point as

$$T_c \sim (p_{Ac} - 0.5)^{-1}. \tag{19}$$

The crossover behavior of the 1d ZPR model has never been addressed in the literature. However, the bicritical

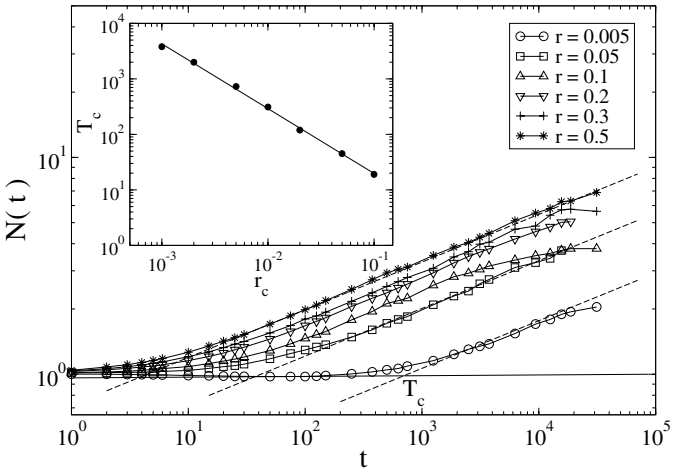

Fig. 5. Log-log of $N(t)$ vs. t obtained at criticality for different values of r_c as indicated in the figure. The time is measured in mcs. The results are averaged over 10^6 different epidemic runs. The horizontal full line shows the expected mean-field behavior ($\eta = 0$), while the dashed-line with slope ($\eta = 0.22$) shows the expected directed percolation behavior. The interception of these lines estimates the crossover time T_c. More details in the text. Inset: Log-log plot of T_c versus r_c. T_c is measured in units of mcs. The straight line shows the best fit of the data obtained using equation (18) that yields a slope $\mu = 1.17$

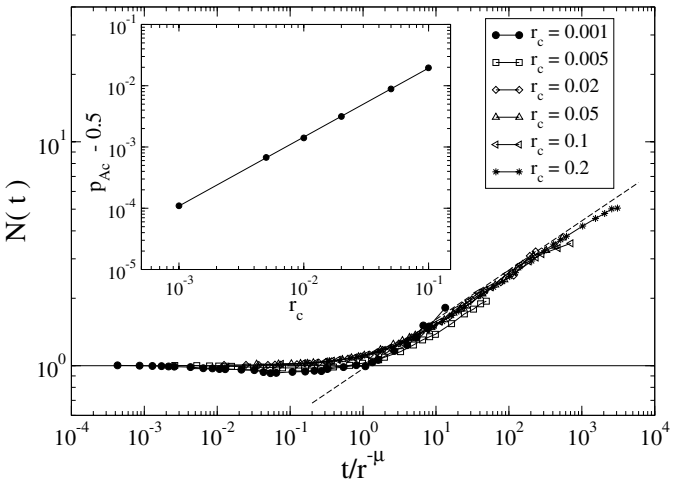

Fig. 6. Log -log plots of $N(t)$ vs. the scaled time (t/T_c) for different values of r_c. Both the time t and T_c are measured in units of mcs. The MF behavior (horizontal full line) and the DP behavior (dashed line) are shown for the sake of comparison. Inset: Log-log plot of p_{Ac} vs. r_c along the border of the active phase in the neighborhood of the bicritical point. The straight line shows the best fit of the data that yields an slope $\phi = 1.13(3)$. $\phi = \mu$ within error bars.

points of the three species monomer-monomer model [17] are in the same universality class as the bicritical point of the 1d ZPR model. Although the authors have not investigated the behavior of the crossover time, they studied the crossover behavior along the border of the active phase and found $\phi \sim 2.1(0.1)$. We expect that in 1d the behavior of the crossover time is also characterized by the

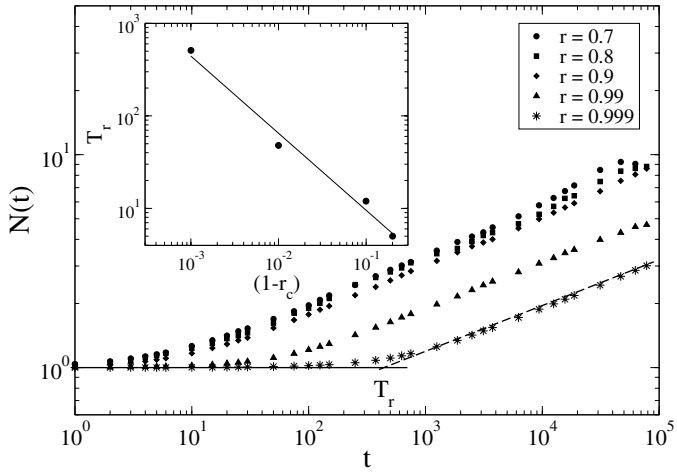

Fig. 7. Log-log of $N(t)$ vs. t obtained at criticality for high values of r_c as indicated in the figure. The time is measured in mcs. The results are averaged over 10^6 different epidemic runs. The flat short-time behavior is similar to that observed for small r, while the asymptotic regime with slope ($\eta = 0.22$) corresponds to the expected directed percolation behavior. The interception of these lines determines the transient time T_r. More details in the text. Inset: Log-log plot of T_r versus $(1-r_c)$. T_r is measured in units of mcs. The straight line shows the best fit of the data that yields an slope $\theta = 0.83(7)$

exponent ϕ which implies that equation (19) should also be valid in $1d$, where instead of 0.5 the actual value of the $1d$ bicritical point should be used.

For high repulsion values, ES become time consuming since another transient behavior similar to the one observed near the bicritical point appears. Figure 7 shows a log-log plot of $N(t)$ versus t where a flat transient behavior is evident before the system reaches the asymptotic regime. In fact, for $r \gtrsim 0.8$ the time T_r needed for the system to reach the asymptotic regime increases. The inset of Figure 7 shows a log-log plot of T_r versus $(1 - r_c)$ where the effect can be observed. Although a power-law behavior could be suggested, more point should be simulated in a region where ES are extremely time consuming. This behavior however can easily be understood after the inspection of typical snapshot configurations obtained for $p_A = 1/2$ and different values of r. In fact, Figure 8a shows a snapshot obtained for $r = 0.2$. In this case, the weak repulsion among adsorbed particles allows the formation of small compact cluster of A and B-species. Increasing the repulsion ($r = 0.8$) in Figure 8b, the formation of compact clusters is no longer observed and, instead the onset of chess-board-like structures of adsorbed species becomes apparent. For the higher repulsion ($r = 0.9$), the configuration of the system is clearly dominated by the chess-board-like structures (see Fig. 8c). Finally, at the border of the phase diagram ($r \simeq 1$ in Fig. 8d) the surface is covered by two shifted chess-board structures with a well defined interface between them. Of course, this a finite-size and finite observation time effect. In fact, for larger lattices one should expect the occurrence of many incompatible chess-board structures. However, as time evolves, a coarsening process is expected to occur such as for the $t \to \infty$ limit a single domain would prevail. It should be noticed that in the bulk of the chess-board structures the occurrence of $A + B \to AB$ reactions has a very small probability which completely vanishes for $r = 1$. So, the bulk is almost inactive and reaction events can only take place along the interfaces between shifted chess-board structures.

It is now possible to understand why the transient behavior observed in Figure 7 is similar to the one shown in Figure 5. Due to the strong repulsion, the almost frozen chessboard patterns develop. Once again, the dynamics of the system is influenced by two equivalent almost absorbing configurations, namely the two shifted chess-board structures that cause the flat transient behavior in the time evolution of $N(t)$. It should be noticed that this effect will occur for strong repulsions as far as $p_A \neq 0, 1$.

Figure 9 shows plots of the coverage of both species (Θ_A and Θ_B), the density of empty sites (Θ_V) and the rate of the AB-reaction (R_{AB}) versus r , respectively. All data correspond to $p_A = p_B = 1/2$. Notice the R_{AB} is given by the number of reaction events per lattice site and unit of time. R_{AB} reaches a broad maximum close to $0.1 \leq r \leq 0.2$ and subsequently decreases smoothly up to $r \simeq 0.85$ where a sudden drop is observed such as $R_{AB} \to 0$ for $r \to 1$. This behavior is in excellent agreement with the set of snapshot configurations already discussed (Fig. 8). In fact, the reduction of R_{AB} is clearly linked to the onset of almost inactive chess-board structures. Also, notice that perfect chess-board structures are characterized by $\Theta_A = \Theta_B = 1/4$ with $\Theta_V = 1/2$ and $R_{AB} \approx 0$, as observed in Figure 9 for $r \to 1$.

Finally, it is worth discussing the nature of the bicritical point and comparing our results for the ZPR model in $d = 2$ with those reported by Zhuo et al. [11] for $d = 1$. For some years, there was an interesting debate concerning the origin of the branching annihilation random walks with even number of offsprings (BAWE) universality class, i.e. why this class was different from the DP class [17–28]. The archetype model which belongs to the BAWE universality class is the BARW model with an even number of offsprings [21,22]. In this model, a local conservation of the number of particles modulo 2 is present. Then, it was argued that this conservation law, which is not present in models that belong to the DP class, was the origin of this new universality class. It should be noted that it is not always straightforward to identify the conserved quantity. In the case of the ZPR model in $1d$, it is not the number of particles but the number of domain walls AVB the conserved modulo 2 quantity at the bicritical point [17]. In addition, there are other models where the number of complex extended objects ("generalized walkers") is the conserved quantity modulo 2 [27,28]. Notice that at the bicritical point the symmetry between the absorbing states emerges. Then, one concludes that the origin of the PC class is either the presence of this symmetry or the conservation of "particles" modulo 2, but both properties should be present. The dynamical renormalization group theory for the BARW with an even number of offsprings indicates that in $1d$ fluctuation effects lead to the emergence of a

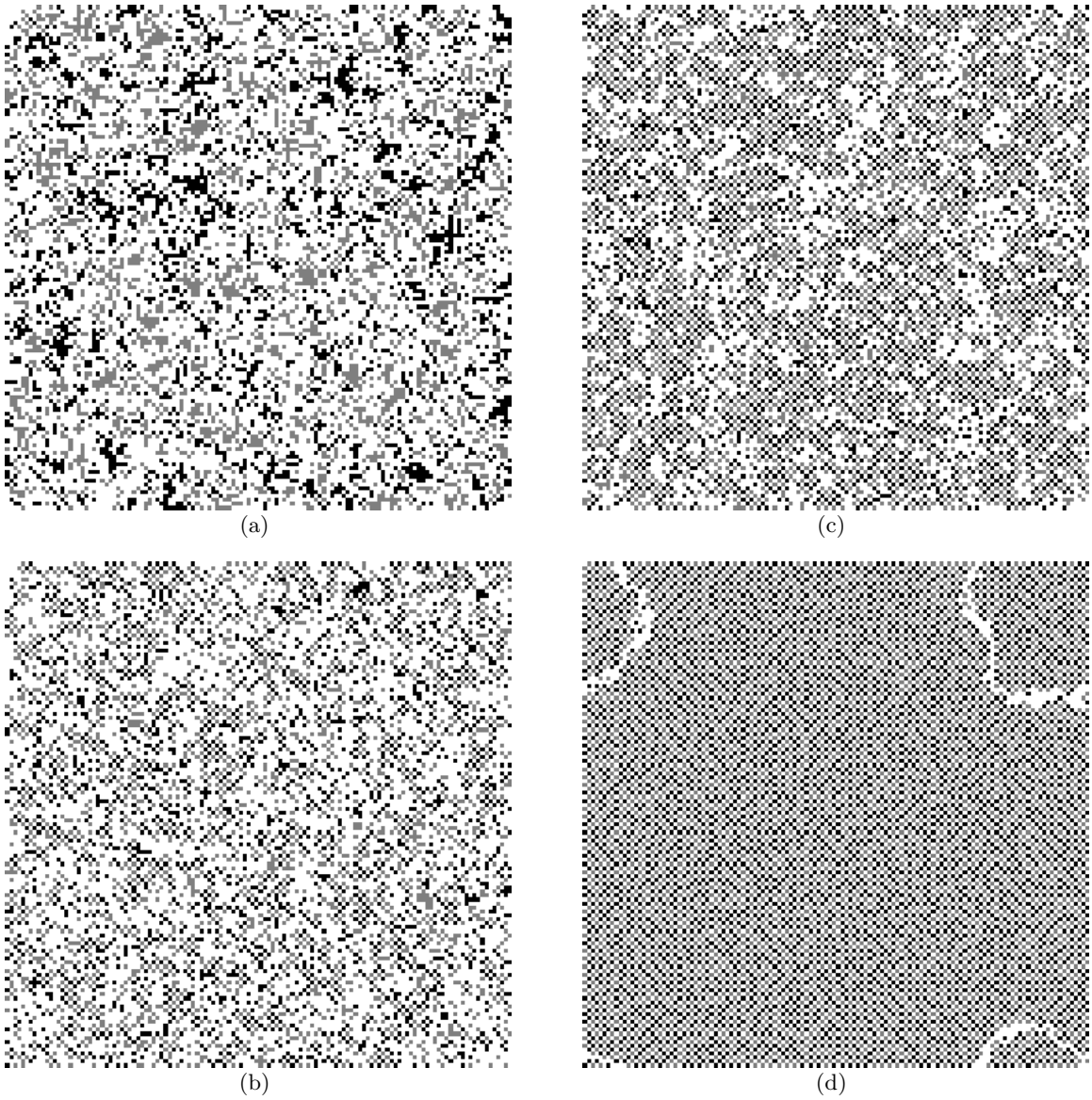

Fig. 8. Typical snapshot configuration obtained for $p_A = 1/2$ and different values of r: a) $r = 0.2$, b) $r = 0.8$, c) $r = 0.9$ and d) $r = 1$. The lattice size is $L = 128$ and the snapshots are taken 1000 mcs after the initialization of the run with empty lattices. Black (gray) squares correspond to $A-$ ($B-$) species while empty sites are left in white.

non-trivial inactive phase for values of the branching rate ($0 \leq \sigma < \sigma_c$) and a dynamic phase transition at σ_c. However, in $2d$ the theory predicts that the critical branching rate takes the value predicted by the mean-field theory $\sigma_c = 0$ [29,30]. In the $1d$ ZPR model, the branching parameter is proportional to the repulsion r and the critical behavior of the model is in complete agreement with this theory since for $p_A = 0.5$ and $r < r_c = 0.2565$ the system displays an inactive phase, while for $p_A = 0.5$ and $r = r_c = 0.2565$ a dynamic phase transition is found. In the $2d$ ZPR model at ($p_A = 0.5, r = 0$), the symmetry between absorbing states emerges but one can not identify pointlike (0 dimensional) walkers as a conserved quantity. Instead, the dynamics is described by a nearly one-dimensional interface whose time evolution forms a tube-like structure. The present model at the bicritical point shares some properties with the so called Voter Model (VM) [31,32], namely the presence of the Z_2 symmetry ($A \to B$) and the same dynamical critical exponents [33]. Although there are still other properties that should be compared like the conservation of a $A(B)$-patch size (analogous to the magnetization in the VM), the absence of surface tension, and the duality [34], this transition is driven by interfacial noise only and consequently the bicritical point belongs to the VM universality class.

It should be noticed that for $r = 0$ (absence of repulsion) the ZPR model is mapped on the standard monomer-monomer (MM) reaction model [5,6,10,35]. So, our results also clarifies the nature of the IPT of the standard MM model that was believed to be of first-order [35].

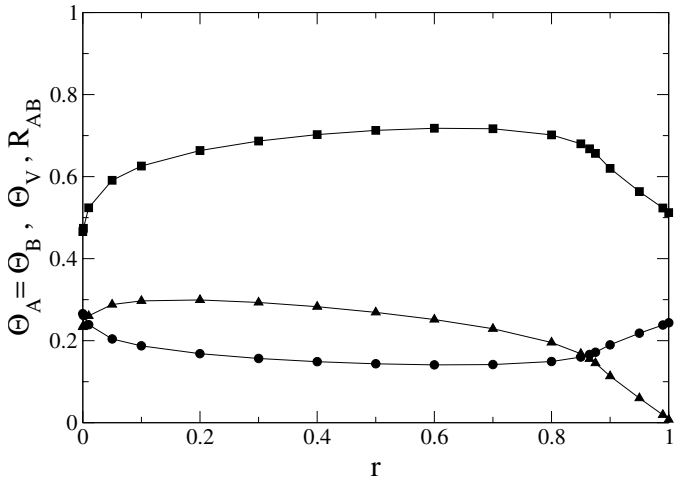

Fig. 9. Plot of $\theta_A = \theta_B$, θ_V and the rate of production of AB-species R_{AB} vs. r. Data obtained for $p_A = p_B = 1/2$ and using lattices of side $L = 256$.

5 Conclusions

We have studied the critical behavior of the ZPR model in 2-d by means of Monte Carlo simulations and a single site mean-field approach. Surprisingly, the simple MF analysis reproduces extremely well the phase diagram found using Monte Carlo simulations. For $r > 0$ the system displays second-order IPT's that belong to the DP universality class. At $(p_A = 0.5, r = 0)$, the symmetry between the absorbing states emerges and the critical behavior is described by dynamical mean-field exponents. This finding suggest that this point belongs to the Voter Model universality class since $d_c = 2$ is the upper critical dimension of this class. The crossover from MF to DP behavior has also been studied. ES in the neighborhood of the bicritical point are influenced by the presence of two equivalent absorbing configurations. For $r \leq 0.1$, the crossover time behaves as a power-law $T_c \sim r^{-\mu}$ with $\mu \approx 1.17(3)$. The same exponent (within error bars) was found for the order of the active phase near the bicritical point which implies that $T_c \sim (p_{Ac} - p_{bic})^{-1}$, where p_{bic} is the value of the bicritical point. We expect that this behavior is also valid in 1d.

For strong repulsions ($r \gtrsim 0.8$), a new transient effect appears due to the presence of metastable long-lived chessboard-like structures. These structures, which are nearly absorbing, prevent the growing of the actual absorbing phase leading to the dramatic increase of the time needed for the system to reach the asymptotic behavior.

This work was supported by CONICET, UNLP and ANPCyT (Argentina).

References

1. R. Imbihl, Prog. Surf. Sci. **44**, 185 (1993)
2. R. Imbihl, G. Ertl, Chem. Rev. **95**, 697 (1995)
3. K. Christmann, *Introduction to Surface Physical Chemistry* (Steinhopff Verlag, Darmstadt 1991)
4. J. Marro, R. Dickman *Nonequilibrium Phase Transitions in Lattice Models* (Cambridge University Press, Cambridge UK, 1999)
5. E.V. Albano, *Surface Chemical Reactions*, in "Computational methods in Surface and Colloid Science" edited by M. Borówko (Marcel Dekker, Inc. New York, 2000), p. 387
6. R. Ziff, E. Gulari, Y. Barshad, Phys. Rev. Lett. **56**, 2553 (1986)
7. K. Yaldram, M.A. Khan, J. Catal. **131**, 369 (1991)
8. E.V. Albano, J. Phys. A. **25**, 2557 (1992)
9. A. Maltz, E.V. Albano, Surf, Sci. **277**, 414 (1992)
10. E.V. Albano, Het. Chem. Rev. **3**, 389 (1996)
11. J. Zhuo, S. Redner, H. Park, J. Phys. A **26**, 4197 (1993)
12. P. Grassberger, A. De la Torre, Ann. Phys. (N.Y.) **122**, 373 (1979)
13. P. Grassberger, J. Phys. A. **22**, 3673 (1989)
14. M.A. Muñoz, R. Dickman, A. Vespignani, S. Zapperi, Phys. Rev. E **59**, 6175 (1999)
15. C.A. Voigt, R.M. Ziff, Phys. Rev. E **56**, R6241 (1997)
16. M.E. Fisher, D.R. Nelson, Phys. Rev. Lett. **32**, 1350 (1974)
17. K.S. Brown, K.E. Bassler, D.A. Brown, Phys. Rev. E **56**, 3953 (1997)
18. P. Grassberger, F. Krause, T. von der Twer, J. Phys. A **17**, L105 (1984)
19. P. Grassberger, J. Phys. A **22**, L1103 (1984)
20. D. ben-Avraham, F. Leyvraz, S. Redner, Phys. Rev. E **50**, 1843 (1994)
21. I. Jensen, J. Phys. A **26**, 3921 (1993)
22. I. Jensen, Phys. Rev. E **50**, 3623 (1994)
23. M.H. Kim, H. Park, Phys. Rev. Lett. **73**, 2579 (1994)
24. H. Park, M.H. Kim, H. Park, Phys. Rev. E **52**, 5664 (1995)
25. H. Park, H. Park, Physica A **221**, 97 (1995)
26. K.E. Bassler, D.A. Brown, Phys. Rev. Lett. **77**, 4094 (1996)
27. H. Hinrichsen, Phys. Rev. E **55**, 219 (1997)
28. R.A. Monetti, Phys. Rev. E **58**, 144 (1998)
29. J.L. Cardy, U.C. Täuber, Phys. Rev. Lett. **77**, 4780 (1996)
30. J.L. Cardy, U.C. Täuber, J. Stat. Phys. **90**, 1 (1998)
31. I. Dornic, H. Chaté, J. Chave, H. Hinrichsen, Phys. Rev. Lett. **87**, 045701 (2001)
32. M. Droz, A. Ferreira, A. Lipowsky, Phys. Rev. E **67**, 056108 (2003)
33. A. Lipowsky, M. Droz, Phys. Rev. E **66**, 016106 (2002)
34. M. Scheucher, H. Spohn, J. Stat. Phys. **53**, 279 (1998)
35. P. Meakin, D.J. Scalapino, J. Chem. Phys. **87**, 731 (1987)